Tuning Membrane Phase Separation Using Nonlipid Amphiphiles

Hari S. Muddana, Homer H. Chiang, and Peter J. Butler*
Department of Bioengineering, The Pennsylvania State University, University Park, Pennsylvania

ABSTRACT Lipid phase separation may be a mechanism by which lipids participate in sorting membrane proteins and facilitate membrane-mediated biochemical signaling in cells. To provide new tools for membrane lipid phase manipulation that avoid direct effects on protein activity and lipid composition, we studied phase separation in binary and ternary lipid mixtures under the influence of three nonlipid amphiphiles, vitamin E (VE), Triton-X (TX)-100, and benzyl alcohol (BA). Mechanisms of additive-induced phase separation were elucidated using coarse-grained molecular dynamics simulations of these additives in a liquid bilayer made from 1,2-dipalmitoyl-*sn*-glycero-3-phosphocholine (DPPC) and 1,2-diundecanoyl-*sn*-glycero-phosphocholine (DUPC). From simulations, the additive's partitioning preference, changes in membrane thickness, and alterations in lipid order were quantified. Simulations showed that VE favored the DPPC phase but partitioned predominantly to the domain boundaries and lowered the tendency for domain formation, and therefore acted as a linactant. This simulated behavior was consistent with experimental observations in which VE promoted lipid mixing and dispersed domains in both gel/liquid and liquid-ordered/liquid-disordered systems. From simulation, BA partitioned predominantly to the DUPC phase, decreased lipid order there, and thinned the membrane. These actions explain why, experimentally, BA promoted phase separation in both binary and ternary lipid mixtures. In contrast, TX, a popular detergent used to isolate raft membranes in cells, exhibited equal preference for both phases, as demonstrated by simulations, but nonetheless, was a strong domain promoter in all lipid mixtures. Further analysis showed that TX increased membrane thickness of the DPPC phase to a greater extent than the DUPC phase and thus increased hydrophobic mismatch, which may explain experimental observation of phase separation in the presence of TX. In summary, these nonlipid amphiphiles provide new tools to tune domain formation in model vesicle systems and could provide the means to form or disperse membrane lipid domains in cells, in addition to the well-known methods involving cholesterol enrichment and sequestration.

INTRODUCTION

Lateral compartmentalization of cell membranes is now a well-recognized modification of the original Singer-Nicholson membrane model (1), and has led to a revolutionized view of how the cell membrane regulates cellular signaling (2,3). A predominant manifestation of lateral compartmentalization of the cell membrane are lipid domains, termed lipid rafts, which are 10 to 100 nm dynamic membrane patches enriched in glycosphingolipids (e.g., sphingomyelin) and cholesterol, and are thought to corral signaling proteins such as small and heterotrimeric G-proteins, nonreceptor tyrosine kinases, and protein phosphatases (2,3), for initiation of signaling cascades at the cell surface (2,4–6). Thus, identifying and understanding the nature of lipid-lipid and lipid-protein intermolecular interactions responsible for domain formation and dynamics in intact cells has now become a fundamental problem in membrane biology (7).

Studies using model membranes and biophysical characterization suggest that domain formation is governed by the interfacial energy between the liquid-ordered (l_o) and liquid-disordered (l_d) domains and the mixing entropy (8). However, significant hurdles remain in the characterization of lipid domain organizing principles in cells, and their physiological significance. First, detection of domains in intact cells under physiological conditions remain challenging due to domains' highly dynamic nature and because their size is below the optical resolution limit of traditional microscopy. Second, available tools for tuning domain formation in cells or model membranes are limited in their ability to control the key driving forces that underlie domain organization and domain-related signal transduction. Important progress on detection of domains in cells was recently made using state-of-the-art single-molecule techniques that confirmed the presence of dynamic domains in intact cells under physiological conditions (9–11). The remaining challenge now is to develop the means to control domain formation/disruption in cells that not only permits studying the role of lipid domains in cell function but also facilitates the development of lipid-domain targeted therapies (12–14).

The predominant experimental tool for controlling lipid domain formation in lipid membranes focuses on altering the concentration of cholesterol using methyl-β-cyclodextrin or statins (15,16) or by depleting cholesterol through enzymatic degradation with cholesterol oxidase (17). Subsequent observations of alterations in signaling cascades or other functions are then interpreted as depending on lipid domains. There are weaknesses in this approach, however.

Submitted March 31, 2011, and accepted for publication December 19, 2011.

*Correspondence: pbutler@psu.edu

Hari S. Muddana's present address is the Skaggs School of Pharmacy and Pharmaceutical Sciences, University of California, San Diego, CA.

Homer H. Chiang's present address is the Department of Chemical Engineering, Massachusetts Institute of Technology, Cambridge, MA.

Editor: Heiko H. Heerklotz.

0006-3495/12/02/0489/9 $2.00

doi: 10.1016/j.bpj.2011.12.033

As pointed out in a review by London (18), association of a membrane process with the concentration of cholesterol is not sufficient to affirm the role of lipid domains, as evidenced by the fact that certain processes, including cholesterol-dependent cytolysins and virus-induced membrane fusion, require high cholesterol concentrations irrespective of the formation of domains. In addition, cholesterol plays multiple structural and functional roles in regulating membrane protein activity that are not dependent on localization of proteins to domains. These include modulating membrane physical properties (e.g., thickness, fluidity, and diffusion) that affect protein conformation and oligomerization (19–21), in addition to modulating lateral organization of the bilayer into lipid domains (16,22). An additional factor complicating the interpretation of cholesterol depletion experiments arises because several membrane proteins, including G-protein-coupled receptors and ligand-gated ion channels, possess specific cholesterol binding sites (23–26) and these specific sterol-protein interactions are thought to be essential for the protein's activity (16,22,27). Thus, there is a need for compounds that alter phase separation in membranes, but do not complex directly with target proteins or alter lipid domain constituents.

One strategy that can result in stabilizing or destabilizing lipid domains, without drastically altering the native membrane composition, is to introduce nonlipid amphiphilic molecules. It is known that addition of flexible and highly unsaturated lipid promotes domain formation (28,29). In a similar manner, at low concentrations, nonionic amphiphiles can preferentially interact and fluidize the l_d regions resulting in domain formation (30). Conversely, compounds that rigidify the l_d regions could lead to mixing of lipids and dissolution of lipid domains. Furthermore, certain hybrid lipids with one saturated chain and one unsaturated chain and other linactants (31) could alter phase separation by modifying interfacial energy at the boundaries (32–34).

We studied phase separation in lipid bilayers under the influence of three nonlipid amphiphiles: α-tocopherol (vitamin E (VE)), Triton-X (TX), and benzyl alcohol (BA) (Fig. 1). Insights into the amphiphile's interaction with lipids, partitioning preference, and the corresponding changes in lipid bilayer physical properties were obtained from coarse-grained (CG) molecular dynamics (MD) simulations of a binary lipid mixture. Experimentally, phase separation was studied in giant unilamellar vesicles prepared from lipid mixtures that resulted in gel-liquid and liquid-liquid phase coexistence.

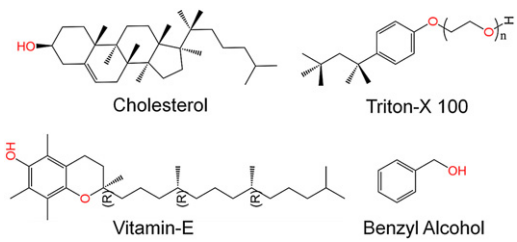

FIGURE 1 Chemical structures of cholesterol, VE, TX-100 ($n = 10$), and BA.

MATERIALS AND METHODS

CGMD simulations

Chemical structures of VE, TX, and BA are shown in Fig. 1. MD simulations were carried out using GROMACS simulation software (version 4.0.3) (35,36). Force fields for lipids, water, and VE/TX/BA were parameterized based on the MARTINI CG model (37,38). Details of CG parameterization and simulation protocol are provided in the Supporting Material. Briefly, all simulations were carried out under constant number, pressure, and temperature conditions with temperature and pressure set to 300 K and 1 bar, respectively (39), for four different systems: pure bilayer (control), and bilayers with VE (10 mol %), TX (10 mol %), and BA (60 mol %). For statistical analysis, trajectories in blocks of 50 ns were analyzed and means and standard errors were computed. A Student's t-test was used to check for statistical significance of changes in bilayer properties due to additives. For order parameters standard errors were <0.002 and standard errors for thickness measurements were <0.02 nm.

Preparation of giant unilamellar vesicles

1,2-dioleoyl-*sn*-glycero-3-phosphocholine (DOPC), 1,2-dipalmitoyl-*sn*-glycero-3-phosphocholine (DPPC), and cholesterol (Chol) were purchased from Avanti Polar Lipids. The fluorescent probe 1,1′-didodecyl-3,3,3′,3′-tetramethylindocarbocyanine perchlorate (DiI-C_{12}; $\lambda_{ex} = 549$ nm; $\lambda_{em} = 565$ nm) was purchased from Invitrogen. BA and α-tocopherol were purchased from Sigma-Aldrich. TX 100 was purchased from MP Biomedicals. All the chemicals were obtained at their highest purity available and used without further purification.

Giant unilamellar vesicles (GUVs) were prepared using the electroformation method (40,41). Lipid mixture solutions were prepared at a concentration of 0.5 mg/ml with a dye concentration of 100 nM. VE and TX at the described mole fractions were added to the lipid mixture solution before preparation of vesicles, whereas BA was added during the hydration of the lipid films. A custom-built electroformation chamber consisting of two transparent indium-tin oxide coverslips was used to apply alternating current electric fields to the lipid film. A silicone spacer of 1.6 mm thickness separated the coverslips. Three to 5 μl of lipid solution was deposited on the coverslips and dried initially under argon for 5 min and then vacuum dried for at least 1 h. The chamber was filled with deionized water preheated to 50°C and moved immediately to a baking oven that was maintained at 50°C. Alternating current electric fields were then applied across the indium-tin oxide electrodes using a LabVIEW controlled A/D board (National Instruments). Applied voltage at 10 Hz frequency was gradually increased from 0.1 V to 1.6 V at a rate of 30 mV/min, followed by a constant voltage of 1.6 V applied for 3 h. Frequency was then reduced to 5 Hz and maintained for 1–2 h to detach the vesicles. A single run of electroformation typically resulted in hundreds of GUVs with sizes ranging from 5 to 100 μm. GUVs were allowed to cool to room temperature for about an hour, before imaging them on an Olympus IX71 inverted microscope equipped with a 60X water-immersion objective and a charge-coupled device camera (Cooke, Romulus, Michigan).

RESULTS AND DISCUSSION

CGMD simulations of a binary lipid mixture with additives

CGMD simulations of a binary lipid mixture (at 300 K) under the influence of VE, TX, and BA, were performed

to determine the additive's phase partitioning preference and the consequent changes in bilayer physical properties. A 1:1 lipid mixture of DPPC and DUPC was chosen for the simulations because the order parameter of doubly unsaturated DUPC is substantially less than that of DPPC (a saturated lipid) and results in liquid-liquid phase separation within the timescale of the CG simulations, which is on the order of 1 μs. Marrink et al. (38) have previously shown that the MARTINI CG model predicts the experimentally determined bilayer thickness of a fluid-phase DPPC bilayer to within 0.2 nm. Chain order parameters from CG simulations were also in very good agreement with atomistic simulations. Moreover, CG has been shown to faithfully simulate other molecules including unsaturated lipids and sterols. Despite the general validity of the MARTINI model in reproducing atomistic simulations, we note that lipid phase transition is not well captured by this model. Specifically, there is no clear indication of gel phase for DPPC lipid as would be expected for the lipid at the simulation temperatures between 283 and 300 K (38). Moreover, even in the crystalline state, no spontaneous tilting of the lipid chains was observed. Complete melting of the crystalline phase was observed starting at 300 K, without any indication of an intermediate gel phase. Due to this limitation in the model, the phase state of the DPPC phase here cannot be defined at 300 K. However, unconstrained lateral mobility of DPPC lipid, and a higher chain ordering of DPPC compared to DUPC in the current study suggests that the DPPC phase state is more reflective of the l_o phase rather than the gel phase. We refer to these phase regions as DPPC phase and DUPC phase in the following discussion. To assess the quality of the CG parameters, we compared the mass-density profiles and order parameters of the different additives to those obtained from atomistic simulations (see Supporting Material). In general, the CG model captured the amphiphilic nature of the additives very well and the corresponding changes in chain ordering were consistent between CG and atomistic simulations.

Snapshots of the bilayer equilibrium conformations with additives obtained from CGMD simulations are shown in Fig. 2, *A–C* (see Supporting Material for the respective side views). Addition of VE and TX had no visually evident change in the domain stabilization or destabilization (Fig. 2, *A* and *B*), whereas, addition of BA resulted in complete separation of the membrane into two domains (Fig. 2 *C*). Quantitatively, we determined the propensity for domain formation by computing the radial pair density distributions of like lipids, i.e., DPPC-DPPC and DUPC-DUPC. Occupancy of DPPC within the first solvation shell of DPPC, which was computed as the ratio of number of DPPC molecules to the number of lipid molecules in the first shell of a DPPC molecule averaged over the trajectory, was used as measure for the tendency of the bilayers to form domains. Occupancy of DPPC >50% indicates preferential interaction of DPPC with itself (i.e., DPPC domain formation). Because smoothly converged radial distribution functions could not be obtained with smaller blocks of trajectories, occupancies were computed as an average over the entire trajectory. In the absence of the additives, the occupancy of DPPC was 68.7%. Addition of VE decreased the occupancy of DPPC by 0.2% to 68.5%, whereas addition of TX and BA increased the occupancy by 0.8% (to 69.5%) and 19.6% (to 88.3%), respectively. This result suggests that VE acts to lower the miscibility temperature, resulting in increased mixing, whereas TX and BA both act to raise the miscibility temperature, and increase phase separation. Thus, despite the modest quantitative changes in the tendency to form domains under the influence of VE and TX, these results qualitatively agree with experimental

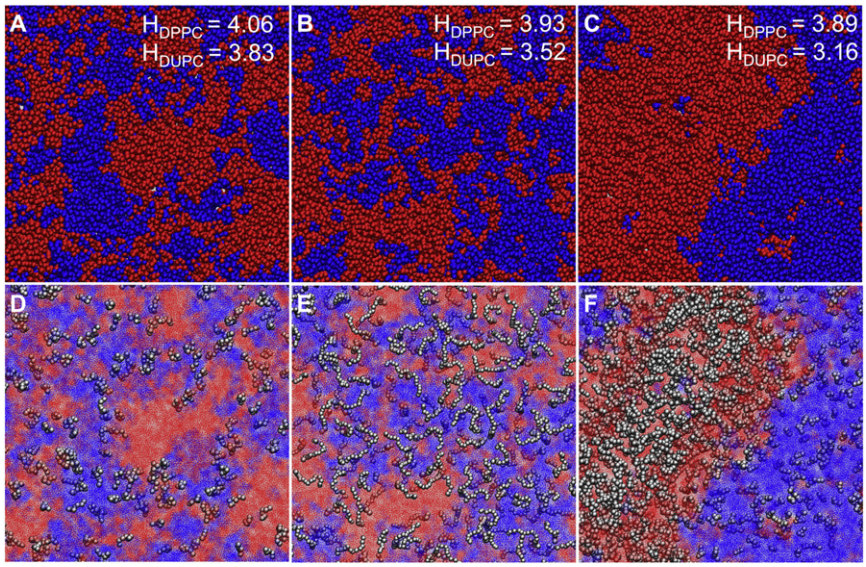

FIGURE 2 (*A–C*) Equilibrium snapshots of a 1:1 lipid mixture of DPPC (*blue*) and DUPC (*red*) bilayer with VE, TX-100, and BA, respectively. For clarity, the additives are not shown in these figures. Thicknesses of the DPPC and DUPC phases in pure bilayer were 3.80 and 3.45 nm, respectively. Simulated lipid distribution without additives was qualitatively similar to simulated lipid distributions in the presence of VE (not shown). Corresponding values in the presence of the additives are shown in the figures. Standard error in thickness is ~0.02 nm. (*D–F*) Distribution of VE, TX, and BA in the same lipid mixture, respectively. DPPC and DUPC lipids are shown in blue and red, respectively, with a dotted representation for clarity. Additives (*gray*) are shown as van der Walls spheres. All simulations were performed at room temperature (300 K) using the MARTINI coarse-grained model.

observations in which VE dispersed domains and TX promoted domain formation in binary lipid mixtures (vida infra).

Mechanism of domain stabilization/destabilization

Influence of an additive on phase separation is dependent on its partitioning preference and also its effect on the relative stability of the phases, which can be quantified using order parameters. Lateral organization of the different additives in the membrane is shown in Fig. 2, *D* and *E*). Partitioning preference of the additives was quantitatively determined by computing the radial pair density distributions between each additive molecule and either DPPC or DUPC molecules (see Fig. 3). Peaks in the radial pair density distribution reflect strong association of the additive with the lipid molecule indicated at the specified distance. VE preferentially associated with DPPC (Fig. 3 *A*), whereas BA preferentially interacted with DUPC (Fig. 3 *C*). TX interacted with DPPC or DUPC with equal propensity (Fig. 3 *B*). Although the radial density distribution suggests VE favored gel phase lipids, visual inspection of Fig. 2 *D* as well as analysis of trajectories during simulations indicated that VE interacted predominantly with domain boundaries. This behavior was further confirmed by the observation that 48% (± 0.2%) of VE molecules had both DPPC and DUPC in VE's first lipid hydration shell. The proportion of VE molecules having only DPPC or only DUPC molecules in the first hydration shell were 36% (± 0.2%) and 16% (± 0.2%), respectively. These findings provide evidence for preferential partitioning of VE to DPPC-DUPC boundaries. Such boundary preference of VE contrasts with the preferential interaction of VE with polyunsaturated fatty acids (42), which prefer liquid domains. However, such preferential interaction is present only when the fatty acid chains possess multiple double bonds and the initial double bond is positioned before the Δ9 position (43) and thus may not be a generalizable phenomenon, or relevant to DUPC, which possesses its double bonds at the 9 and 12 positions. On the other hand, BA was predominately found in the DUPC phase, distributed uniformly across this region, a finding that is consistent with previous observations that primary alcohols partition preferentially to liquid-phase domains (44). In our simulations, TX was found to be partitioned equally between the two phases, which is also in agreement with previous experimental observations of TX partitioning equally in bilayers composed of POPC and sphingomyelin (45,46). It is worth noting that TX partitions favorably in the l_d regions in the presence of cholesterol, due to strong unfavorable interaction between cholesterol and TX (45,47), which suggests that cholesterol might also play an important role in determining the partitioning of the additive.

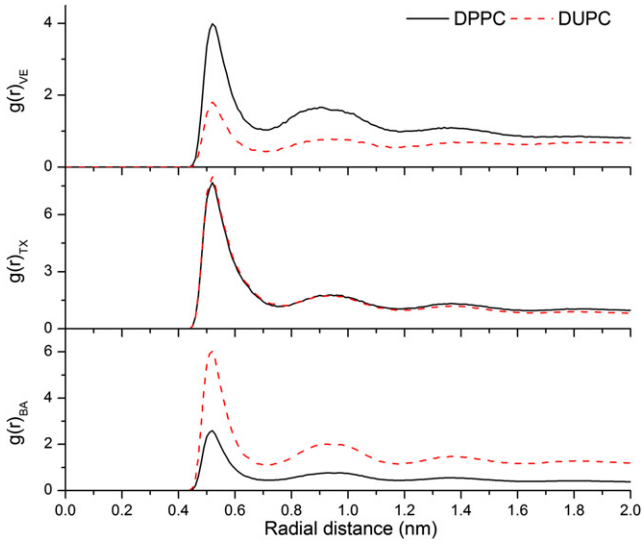

FIGURE 3 (*Top* to *bottom*) Radial pair density distributions of DPPC (*black*, *solid*) and DUPC (*red*, *dashed*) molecules with reference to VE (*top*), TX (*middle*), and BA (*bottom*) molecules.

To assess the ordering of different phases in the presence of additives, we computed the chain order parameters of DPPC and DUPC lipids, averaged over both chains as described previously (38,48). Relative changes in the ordering (which is directly correlated to membrane thickness) of the two phases could raise or lower the miscibility temperature. Changes in order parameter along the lipid acyl chains in the presence of additives relative to the pure bilayer are shown in Fig. 4. VE is known to increase (or decrease) the ordering of the fluid (or gel) phase, similar to cholesterol (49). Addition of VE induced a slight, but statistically significant increase in the order of the DPPC phase and a slight decrease in the DUPC phase, which is explained by VE's preference to favor partitioning to the domain boundaries over the domains themselves. The presence of VE at the domain interface might contribute to lowering the interfacial energy, and thereby lower the miscibility temperature. On the other hand, BA induced significant disordering of the DUPC phase relative to the DUPC phase, whereas TX induced a slight ordering of the DPPC phase relative to the DUPC phase. This result was expected for BA, which partitions preferentially into the fluid phase (44). However, the relative increase in ordering of the DPPC phase upon addition of TX was not expected, given the observation that TX is uniformly distributed in the membrane. In either case, disordering of the DUPC phase relative to the DPPC phase or ordering of the DPPC phase relative to the DUPC phase would contribute to an increase in height mismatch at the domain boundaries, which in turn contributes positively to the phase separation.

We further determined the thickness mismatch by computing the thickness of DPPC and DUPC phases under

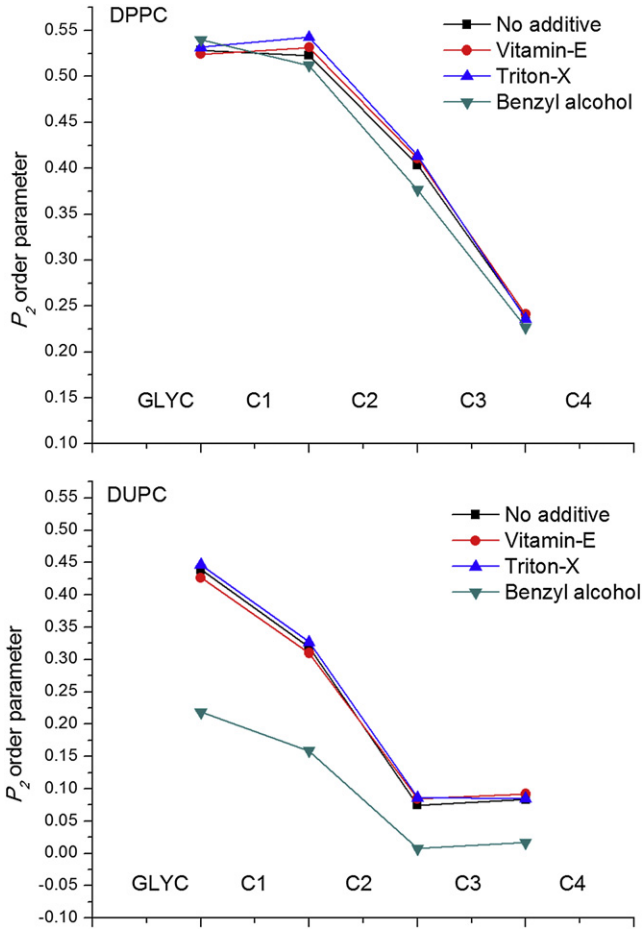

FIGURE 4 P_2 order parameter of the consecutive bonds of DPPC and DUPC molecules. Chain order parameters were averaged over both the chains. Standard errors (not shown) are <0.002.

the influence of the previous additives. Local thickness of the membrane was computed as the distance between the phosphate groups of the two leaflets, averaged over the trajectory. Standard errors in thickness measurements were <0.02 nm. Thickness of the DPPC and DUPC phases in the pure bilayer were 3.80 and 3.45 nm, respectively, with a thickness mismatch of 0.35 nm. Addition of VE resulted in an increase in the thickness of both DPPC and DUPC phases to 4.06 and 3.83 nm, respectively, thereby lowering the thickness mismatch to 0.23 nm. Addition of TX increased the thickness of DPPC and DUPC phases to 3.93 and 3.52, respectively, resulting in an increased mismatch of 0.41 nm. Similarly, addition of BA increased the thickness of the DPPC phase to 3.89 nm and dramatically decreased the thickness of the DUPC phase to 3.16 nm, resulting in an increase in thickness mismatch of 0.73 nm. These results strongly support the idea that each of the additives promoted (or disrupted) membrane phase separation by increasing (or lowering) lipid-lipid height mismatch, which in turn could contribute to an increase (or decrease) in interfacial energy.

Lateral phase separation in ternary mixtures of DOPC, DPPC, and Chol/VE/TX/BA

Effects of membrane additives on lateral phase separation were determined experimentally in giant unilamellar vesicles made from ternary and quaternary (see next section) mixtures of DOPC, DPPC, cholesterol, and VE/TX/BA. Phases were observed using fluorescence microscopy of vesicles containing DiI-C_{12}, a short chain fluorescence probe that preferentially partitions into the liquid phase under gel-liquid phase coexistence and to l_d regions under liquid-liquid phase coexistence (50,51). Gel-liquid and liquid-liquid phase coexistence was inferred from the fluorescence images based on morphology of the domains. For example, liquid-liquid coexisting phases exhibit circular morphology, whereas gel-liquid coexisting phases exhibit irregular domain morphology (52). A 1:1 binary mixture of DOPC and DPPC in the absence of any other additives exhibited gel-liquid coexisting phase regions, as shown in Fig. 5 *A*, with DOPC in the liquid region and DPPC in the gel region. We determined the domain morphologies in this lipid mixture under the influence of different additives. VE and TX were added to the lipid stock solutions before the preparation of GUVs at the stated molar concentrations. Because preparation of GUVs using electroformation involves completely drying the solvent (chloroform) before

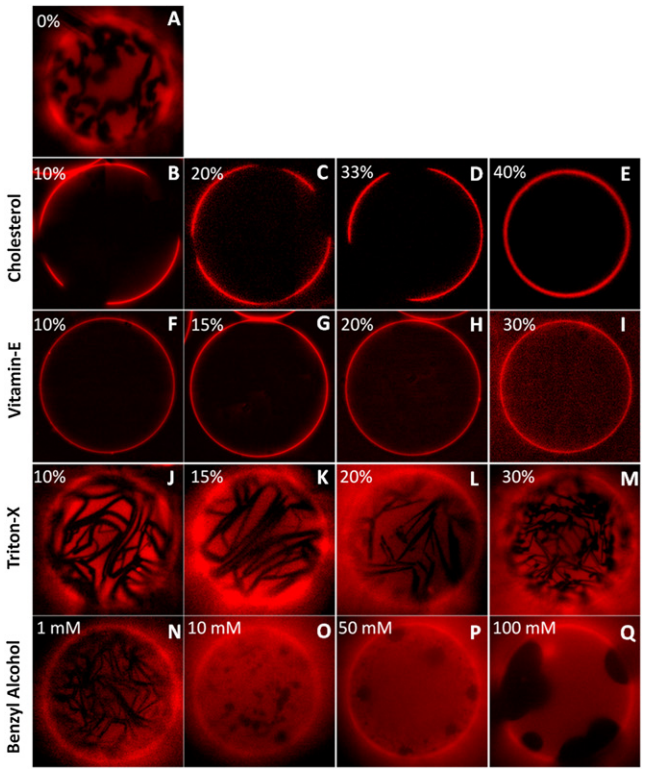

FIGURE 5 (*A*) Gel-liquid coexisting phases in 1:1 DOPC/DPPC lipid mixture. Phase separation behavior in 1:1 DOPC/DPPC mixture under the influence of cholesterol (*B–E*), VE (*F–I*), TX-100 (*J–M*), and BA (*N–Q*). Experiments were carried out at room temperature.

hydration, BA, which would evaporate during this process, was added to the lipid bilayer after rehydration. Note that the concentrations shown in Figs. 4 and 5 represent the mole fractions in the stock lipid solutions used during the preparation of the GUVs, and do not account for the partitioning of the additive between the membrane and water. Estimates of the additive concentration in the membrane can be obtained from the lipid concentration (~15 μM) and the additive's membrane-water partitioning coefficient. Octanol-water partition coefficients (logP) of VE, TX, and BA, predicted using the XLOGP3 algorithm (53) were 10.7, 4.6, and 1.1, respectively, which result in membrane partitioning of 99.9%, 1.1%, and 10^{-6}% of VE, TX, and BA, respectively. Because these estimates are based on the partition coefficients between octanol and water, they represent the fractions found in the hydrophobic core of the membrane, and therefore are not likely to be accurate for molecules (e.g., TX and BA) that primarily partition to the lipid-water interface.

Phase separation in ternary mixtures of DOPC, DPPC, and cholesterol has been studied extensively in the past, and so served here as a positive control (52,54). Addition of cholesterol in the range of 10 mol% to 30 mol% resulted in coexisting liquid phases (Fig. 5, *B–E*). Beyond 40 mol% cholesterol, no lateral phase separation was observed. These results are consistent with phase diagrams of DOPC/DPPC/cholesterol reported by others (52). Despite the similarity in structure of VE and cholesterol (shown in Fig. 1), the phase separation behavior upon addition of VE differs significantly from that of cholesterol. First, coexisting liquid-liquid phases were not observed at any concentration of VE, up to 30%. Addition of VE, even at the lowest concentration studied (10 mol%), resulted in complete disruption of gel-liquid coexistence. Beyond 30% VE, giant vesicles could not be formed likely because the inverted-cone-like structure of VE induces formation of micelles that prevent larger scale bilayer formation. The question arises of why VE dramatically reverses phase separation induced by cholesterol. Previous studies have shown that cholesterol partitions preferentially with gel phase lipid because of its high affinity for fully saturated lipids (55,56). According to the umbrella model, (57) lipid polar headgroups cover the bulky hydrophobic tetrameric ring of the cholesterol molecule, and saturated lipids provide better coverage than do unsaturated lipids (58), contributing to the preferential interaction of cholesterol with saturated lipids in lipid mixtures. Unlike cholesterol, VE has a more flexible and less bulky hydrophobic tail region resulting in its high conformational flexibility. Although VE slightly favored interaction with the gel phase lipid (as seen in CGMD simulations), it is predominantly partitioned at the domain boundaries, thereby acting as a linactant. This difference in partitioning and the consequent effects on lipid-lipid interfacial energy might explain the observed differences in phase separation behavior with cholesterol and VE.

On the other hand, addition of TX or BE consistently resulted in phase coexistence in 1:1 DOPC/DPPC mixture (Fig. 5). However, we noticed some differences in domain morphologies resulting from these two additives. Domain morphologies in the case of TX were similar to those observed in pure gel-liquid coexistence (Fig. 5 *A*). However, in the case of BA, domain morphologies resembled liquid-liquid coexisting regions and domains increased in size with increasing concentrations of BA (Fig. 5, *N–Q*). In fact, at the highest concentration (100 mM), BA resulted in significantly larger domains (Fig. 5 *Q*). The persistence of gel phase domains in the presence of TX indicates that TX does not perturb the packing in gel phase regions significantly, contrary to simulations. This is likely a limitation of the coarse-grained model in which no clear gel phase was simulated, thus allowing penetration of TX into both phases. Induction of liquid-liquid phase coexistence by BA indicates that it perturbs the packing in both gel and liquid-phase regions. If BA were to interact preferentially with gel phase lipids, then it would perturb the ordering of the gel phase regions more than that of the fluid phase region, thereby promoting lipid mixing. However, this is not what was observed in experiments in which increases in concentration of BA promoted even larger domain formation. Therefore, we conclude that BA interacts favorably with the fluid-phase lipid and promotes phase separation, consistent with the simulations. In fact, these results suggest that alcohols and commonly used anesthetics might exert their effect by promoting lipid domain formation in vivo.

Lateral phase separation in quaternary mixtures of DOPC, DPPC, Cholesterol, and VE/TX/BA

Membrane rafts in intact cells closely resemble liquid-liquid coexisting phase domains exhibited by ternary lipid mixtures (two lipids and cholesterol) (59). To understand how these membrane additives influence lipid mixing in the presence of cholesterol, we studied lateral phase separation behavior in two different lipid mixtures: (Mixture 1) 1:1:0.7 DOPC/DPPC/Chol that forms coexisting liquid-liquid membranes, and (Mixture 2) 1:1:1.2 DOPC/DPPC/Chol that forms homogeneous liquid phase membranes, under the influence of the different additives. These lipid compositions were chosen so that they are close to the boundary (above and below) of the liquid-liquid phase coexistence region in the phase diagram (52).

Giant vesicles prepared from Mixture 1 consistently exhibited liquid-liquid phase separation (Fig. 6 *A*). Addition of VE to this mixture resulted in a microscopically uniform mixed phase (Fig. 6, *B* and *C*), implying that VE acts to lower the miscibility temperature, which is consistent with the observed behavior in binary mixtures (Fig. 5). On the other hand, giant vesicles prepared from Mixture 2 exhibit no phase separation due to the high concentration

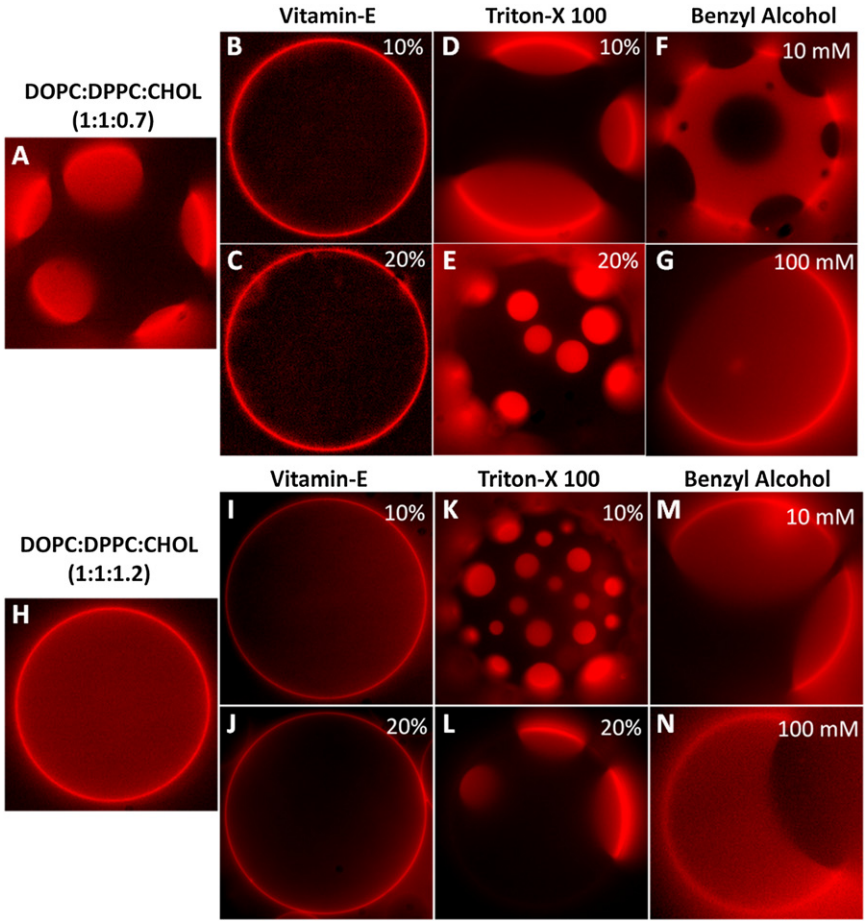

FIGURE 6 (*A*) Liquid-liquid phase coexistence in 1:1:0.7 DOPC/DPPC/Chol GUVs. Phase separation behavior of mixture in *A* under the influence of VE (*B* and *C*), TX-100 (*D* and *E*), and BA (*F* and *G*). (*H*) Single-phase GUVs prepared from 1:1:1.2 DOPC/DPPC/Chol. Phase separation behavior of mixture in *H* under the influence of VE (*I* and *J*), TX-100 (*K* and *L*), and BA (*M* and *N*). Experiments were carried out at room temperature.

of cholesterol (see Fig. 6 *H*). No change in the phase mixing state was observed with the addition of VE (see Fig. 6, *I* and *J*), implying that VE does not raise the miscibility temperature. This result is similar to that observed with cholesterol, where further addition of cholesterol to homogeneous liquid phase vesicles (above 30–40% cholesterol) does not alter the phase state (52).

Both TX and BA promoted or stabilized domain formation. Addition of TX to Mixture 1 (with preexisting domains) did not alter the coexisting liquid-liquid phases (Fig. 6, *D* and *E*), whereas addition of BA induced even larger domain formation at high concentrations (Fig. 6, *F* and *G*), similar to that observed in binary lipid mixtures. That is, phase coexistence was sustained under the influence of these additives. These results together with the results outlined in previous sections also indicate that BA has a stronger influence on lipid mixing/demixing than TX. In Mixture 2, addition of TX and BA each acted to raise the miscibility temperature and promoted the formation of liquid-liquid coexisting regions (Fig. 6, *K–N*), suggesting that both these amphiphiles drive domain formation, an effect that is exactly opposite to that of VE. We even observed reversible phase separation by adding VE and TX sequentially. That is, addition of VE first resulted in uniform mixing of the lipids, and further addition of TX to this membrane reversed the effect of VE by inducing the formation of domains (Fig. 7). In summary, these results suggest that the observed effect of the different additives on phase separation in the presence of cholesterol is qualitatively similar to that in binary lipid mixtures, and the mechanism of action might be similar in both the cases.

CONCLUSIONS

Several recent experimental and theoretical studies point to interfacial forces originating from interactions at the l_d and l_o phase boundaries as a key determinant of domain formation (8,60–63). A variety of factors contribute to the interfacial free-energy (both enthalpic and entropic) including hydrophobic mismatch, spontaneous curvature, and dipole density (64,65). Coalescence of small domains to form larger domains minimizes the interfacial free-energy due to reduction in boundary length; however, this coalescence is opposed by the mixing entropy. From our results, predominant partitioning of VE to the domain boundaries and the decreased tendency to form domains, suggests that VE acts to decrease the interfacial free-energy. On the other

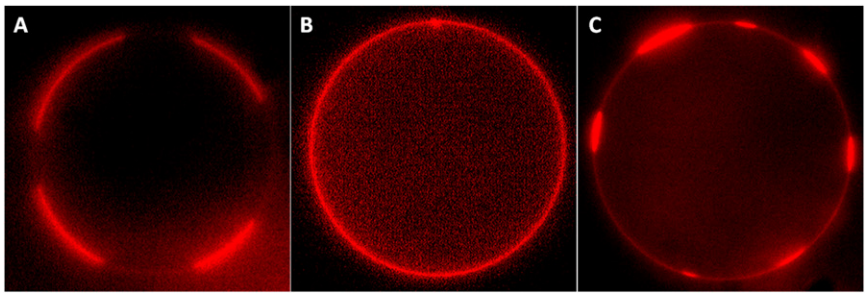

FIGURE 7 (*A*) Phase separation in GUVs prepared from DOPC/DPPC/Chol (35:35:30). (*B*) Addition of 20 mol% VE resulted in disruption of phase partitioning. (*C*) Addition of 20 mol% TX to DOPC/DPPC/Chol (35:35:30) + 20% VE GUVs resulted in repartitioning of the phases. Experiments were carried out at room temperature.

hand, BA predominantly partitions to the disordered phase, decreases membrane thickness, and increases hydrophobic mismatch, which in turn contributes to an increase in interfacial energy at domain boundaries. Similarly, despite its uniform partitioning across the phases, TX increases the order of the ordered phase more than it does for the disordered phase, thereby increasing the interfacial energy at domain boundaries, which leads to phase separation. These results, together, suggest that nonlipid amphiphiles contribute to phase separation by increasing or decreasing interfacial energy. Further studies are required to determine if these additives can tune lipid domain formation in cell membranes. Such behavior would have a significant impact in understanding lipid phase control of cellular biochemical and mechanobiological signaling (66,67).

SUPPORTING MATERIAL

Additional simulations, validations, four figures, and references are available at http://www.biophysj.org/biophysj/supplemental/S0006-3495(11)05462-2.

The authors acknowledge helpful discussions with Dr. Evangelos Manias (The Pennsylvania State University) and Dr. Tristan Tabouillot (University of Michigan).

This work was supported by grants to P.J.B. from the National Heart Lung and Blood Institute (R01 HL 07754201) and the National Science Foundation (BES 0238910).

REFERENCES

1. Singer, S. J., and G. L. Nicolson. 1972. The fluid mosaic model of the structure of cell membranes. *Science.* 75:720–731.
2. Pike, L. J. 2003. Lipid rafts: bringing order to chaos. *J. Lipid Res.* 44:655–667.
3. Pike, L. J. 2006. Rafts defined: a report on the Keystone Symposium on Lipid Rafts and Cell Function. *J. Lipid Res.* 47:1597–1598.
4. Simons, K., and D. Toomre. 2000. Lipid rafts and signal transduction. *Nat. Rev. Mol. Cell Biol.* 1:31–39.
5. Simons, K., and E. Ikonen. 1997. Functional rafts in cell membranes. *Nature.* 387:569–572.
6. Bethani, I., S. S. Skånland, I. Dikic, and A. Acker-Palmer. 2010. Spatial organization of transmembrane receptor signalling. *EMBO J.* 29:2677–2688.
7. Jacobson, K., O. G. Mouritsen, and R. G. W. Anderson. 2007. Lipid rafts: at a crossroad between cell biology and physics. *Nat. Cell Biol.* 9:7–14.
8. Pike, L. J. 2009. The challenge of lipid rafts. *J. Lipid Res.* 50 (*Suppl*):S323–S328.
9. Sahl, S. J., M. Leutenegger, …, C. Eggeling. 2010. Fast molecular tracking maps nanoscale dynamics of plasma membrane lipids. *Proc. Natl. Acad. Sci. USA.* 107:6829–6834.
10. Eggeling, C., C. Ringemann, …, S. W. Hell. 2009. Direct observation of the nanoscale dynamics of membrane lipids in a living cell. *Nature.* 457:1159–1162.
11. Ringemann, C., B. Harke, …, C. Eggeling. 2009. Exploring single-molecule dynamics with fluorescence nanoscopy. *N. J. Phys.* 11: 103054.
12. Zhuang, L. Y., J. Kim, …, M. R. Freeman. 2005. Cholesterol targeting alters lipid raft composition and cell survival in prostate cancer cells and xenografts. *J. Clin. Invest.* 115:959–968.
13. Mollinedo, F., J. de la Iglesia-Vicente, …, M. J. Blanco-Prieto. 2010. Lipid raft-targeted therapy in multiple myeloma. *Oncogene.* 29:3748–3757.
14. Mollinedo, F., and C. Gajate. 2010. Lipid rafts and clusters of apoptotic signaling molecule-enriched rafts in cancer therapy. *Future Oncol.* 6:811–821.
15. Zidovetzki, R., and I. Levitan. 2007. Use of cyclodextrins to manipulate plasma membrane cholesterol content: evidence, misconceptions and control strategies. *Biochim. Biophys. Acta.* 1768:1311–1324.
16. Pucadyil, T. J., and A. Chattopadhyay. 2006. Role of cholesterol in the function and organization of G-protein coupled receptors. *Prog. Lipid Res.* 45:295–333.
17. Samsonov, A. V., I. Mihalyov, and F. S. Cohen. 2001. Characterization of cholesterol-sphingomyelin domains and their dynamics in bilayer membranes. *Biophys. J.* 81:1486–1500.
18. London, E. 2005. How principles of domain formation in model membranes may explain ambiguities concerning lipid raft formation in cells. *Biochim. Biophys. Acta.* 1746:203–220.
19. Botelho, A. V., T. Huber, …, M. F. Brown. 2006. Curvature and hydrophobic forces drive oligomerization and modulate activity of rhodopsin in membranes. *Biophys. J.* 91:4464–4477.
20. Lee, A. G. 2004. How lipids affect the activities of integral membrane proteins. *Biochim. Biophys. Acta.* 1666:62–87.
21. Periole, X., T. Huber, …, T. P. Sakmar. 2007. G protein-coupled receptors self-assemble in dynamics simulations of model bilayers. *J. Am. Chem. Soc.* 129:10126–10132.
22. Yeagle, P. 2005. The Structure of Biological Membranes. CRC Press, Boca Raton, FL.
23. Paila, Y. D., S. Tiwari, and A. Chattopadhyay. 2009. Are specific nonannular cholesterol binding sites present in G-protein coupled receptors? *Biochim. Biophys. Acta.* 1788:295–302.
24. Paila, Y. D., and A. Chattopadhyay. 2009. The function of G-protein coupled receptors and membrane cholesterol: specific or general interaction? *Glycoconj. J.* 26:711–720.
25. Hanson, M. A., V. Cherezov, …, R. C. Stevens. 2008. A specific cholesterol binding site is established by the 2.8 A structure of the human beta2-adrenergic receptor. *Structure.* 16:897–905.

26. Jones, O. T., and M. G. McNamee. 1988. Annular and nonannular binding sites for cholesterol associated with the nicotinic acetylcholine receptor. *Biochemistry.* 27:2364–2374.
27. Burger, K., G. Gimpl, and F. Fahrenholz. 2000. Regulation of receptor function by cholesterol. *Cell. Mol. Life Sci.* 57:1577–1592.
28. Bakht, O., P. Pathak, and E. London. 2007. Effect of the structure of lipids favoring disordered domain formation on the stability of cholesterol-containing ordered domains (lipid rafts): identification of multiple raft-stabilization mechanisms. *Biophys. J.* 93:4307–4318.
29. Wassall, S. R., M. R. Brzustowicz, …, W. Stillwell. 2004. Order from disorder, corralling cholesterol with chaotic lipids. The role of polyunsaturated lipids in membrane raft formation. *Chem. Phys. Lipids.* 132:79–88.
30. Heerklotz, H. 2008. Interactions of surfactants with lipid membranes. *Q. Rev. Biophys.* 41:205–264.
31. Trabelsi, S., S. Zhang, …, D. K. Schwartz. 2008. Linactants: surfactant analogues in two dimensions. *Phys. Rev. Lett.* 100:037802.
32. Brewster, R., and S. A. Safran. 2010. Line active hybrid lipids determine domain size in phase separation of saturated and unsaturated lipids. *Biophys. J.* 98:L21–L23.
33. Brewster, R., P. A. Pincus, and S. A. Safran. 2009. Hybrid lipids as a biological surface-active component. *Biophys. J.* 97:1087–1094.
34. Schäfer, L. V., and S. J. Marrink. 2010. Partitioning of lipids at domain boundaries in model membranes. *Biophys. J.* 99:L91–L93.
35. Van Der Spoel, D., E. Lindahl, …, H. J. Berendsen. 2005. GROMACS: fast, flexible, and free. *J. Comput. Chem.* 26:1701–1718.
36. Lindahl, E., B. Hess, and D. van der Spoel. 2001. GROMACS 3.0: a package for molecular simulation and trajectory analysis. *J. Mol. Model.* 7:306–317.
37. Marrink, S. J., H. J. Risselada, …, A. H. de Vries. 2007. The MARTINI force field: coarse grained model for biomolecular simulations. *J. Phys. Chem. B.* 111:7812–7824.
38. Marrink, S. J., A. H. de Vries, and A. E. Mark. 2004. Coarse grained model for semiquantitative lipid simulations. *J. Phys. Chem. B.* 108: 750–760.
39. Berendsen, H. J. C., J. P. M. Postma, …, J. R. Haak. 1984. Molecular-dynamics with coupling to an external bath. *J. Chem. Phys.* 81:3684–3690.
40. Angelova, M. I., and D. S. Dimitrov. 1986. Liposome electroformation. *Faraday Discuss. Chem. Soc.* 81:303–311.
41. Estes, D. J., and M. Mayer. 2005. Electroformation of giant liposomes from spin-coated films of lipids. *Colloids Surf. B Biointerfaces.* 42: 115–123.
42. Ortiz, A., F. J. Aranda, and J. C. Gómez-Fernández. 1987. A differential scanning calorimetry study of the interaction of alpha-tocopherol with mixtures of phospholipids. *Biochim. Biophys. Acta.* 898:214–222.
43. Stillwell, W., T. Dallman, …, L. J. Jenski. 1996. Cholesterol versus alpha-tocopherol: effects on properties of bilayers made from heteroacid phosphatidylcholines. *Biochemistry.* 35:13353–13362.
44. Terama, E., O. H. S. Ollila, …, I. Vattulainen. 2008. Influence of ethanol on lipid membranes: from lateral pressure profiles to dynamics and partitioning. *J. Phys. Chem. B.* 112:4131–4139.
45. Tsamaloukas, A., H. Szadkowska, and H. Heerklotz. 2006. Nonideal mixing in multicomponent lipid/detergent systems. *J. Phys. Condens. Matter.* 18:S1125–S1138.
46. Arnulphi, C., J. Sot, …, F. M. Goñi. 2007. Triton X-100 partitioning into sphingomyelin bilayers at subsolubilizing detergent concentrations: effect of lipid phase and a comparison with dipalmitoylphosphatidylcholine. *Biophys. J.* 93:3504–3514.
47. Heerklotz, H., H. Szadkowska, …, J. Seelig. 2003. The sensitivity of lipid domains to small perturbations demonstrated by the effect of Triton. *J. Mol. Biol.* 329:793–799.
48. Gullapalli, R. R., M. C. Demirel, and P. J. Butler. 2008. Molecular dynamics simulations of DiI-C18(3) in a DPPC lipid bilayer. *Phys. Chem. Chem. Phys.* 10:3548–3560.
49. Atkinson, J., R. F. Epand, and R. M. Epand. 2008. Tocopherols and tocotrienols in membranes: a critical review. *Free Radic. Biol. Med.* 44:739–764.
50. Klausner, R. D., and D. E. Wolf. 1980. Selectivity of fluorescent lipid analogues for lipid domains. *Biochemistry.* 19:6199–6203.
51. Baumgart, T., G. Hunt, …, G. W. Feigenson. 2007. Fluorescence probe partitioning between L-o/L-d phases in lipid membranes. *Biochim. Biophys. Acta.* 1768:2182–2194.
52. Veatch, S. L., and S. L. Keller. 2003. Separation of liquid phases in giant vesicles of ternary mixtures of phospholipids and cholesterol. *Biophys. J.* 85:3074–3083.
53. Cheng, T. J., Y. Zhao, …, L. Lai. 2007. Computation of octanol-water partition coefficients by guiding an additive model with knowledge. *J. Chem. Inf. Model.* 47:2140–2148.
54. Feigenson, G. W., and J. T. Buboltz. 2001. Ternary phase diagram of dipalmitoyl-PC/dilauroyl-PC/cholesterol: nanoscopic domain formation driven by cholesterol. *Biophys. J.* 80:2775–2788.
55. Niu, S. L., and B. J. Litman. 2002. Determination of membrane cholesterol partition coefficient using a lipid vesicle-cyclodextrin binary system: effect of phospholipid acyl chain unsaturation and headgroup composition. *Biophys. J.* 83:3408–3415.
56. Risselada, H. J., and S. J. Marrink. 2008. The molecular face of lipid rafts in model membranes. *Proc. Natl. Acad. Sci. USA.* 105:17367–17372.
57. Huang, J. Y., and G. W. Feigenson. 1999. A microscopic interaction model of maximum solubility of cholesterol in lipid bilayers. *Biophys. J.* 76:2142–2157.
58. Ali, M. R., K. H. Cheng, and J. Y. Huang. 2007. Assess the nature of cholesterol-lipid interactions through the chemical potential of cholesterol in phosphatidylcholine bilayers. *Proc. Natl. Acad. Sci. USA.* 104:5372–5377.
59. Simons, K., and W. L. C. Vaz. 2004. Model systems, lipid rafts, and cell membranes. *Annu. Rev. Biophys. Biomol. Struct.* 33:269–295.
60. Kuzmin, P. I., S. A. Akimov, …, F. S. Cohen. 2005. Line tension and interaction energies of membrane rafts calculated from lipid splay and tilt. *Biophys. J.* 88:1120–1133.
61. Akimov, S. A., V. A. Frolov, and P. I. Kuzmin. 2005. Line tension and size distribution function of nanorafts in bilayer lipid membranes. *Biologicheskie Membrany.* 22:413–426.
62. Akimov, S. A., and P. I. Kuzmin. 2005. Line tension of raft/surround monolayer boundary calculated from splay, tilt and area compression/stretching. *Biologicheskie Membrany.* 22:137–146.
63. García-Sáez, A. J., S. Chiantia, and P. Schwille. 2007. Effect of line tension on the lateral organization of lipid membranes. *J. Biol. Chem.* 282:33537–33544.
64. Lee, D. W., Y. J. Min, …, J. A. Zasadzinski. 2011. Relating domain size distribution to line tension and molecular dipole density in model cytoplasmic myelin lipid monolayers. *Proc. Natl. Acad. Sci. USA.* 108:9425–9430.
65. Baumgart, T., S. T. Hess, and W. W. Webb. 2003. Imaging coexisting fluid domains in biomembrane models coupling curvature and line tension. *Nature.* 425:821–824.
66. Tabouillot, T., H. S. Muddana, and P. J. Butler. 2011. Endothelial cell membrane sensitivity to shear stress is lipid domain dependent. *Cellular and Molecular Bioengineering.* 4:169–181.
67. Muddana, H. S., R. R. Gullapalli, …, P. J. Butler. 2011. Atomistic simulation of lipid and DiI dynamics in membrane bilayers under tension. *Phys. Chem. Chem. Phys.* 13:1368–1378.